Combined simulation of quasi-static deep drawing and electromagnetic forming by means of a coupled damage–viscoplasticity model at finite strains

Y. Kiliclar[1], O. K. Demir[2], I. N. Vladimirov[1], L. Kwiatkowski[2], A. Brosius[2], S. Reese[1], A. E. Tekkaya[2]

[1] Institute of Applied Mechanics, RWTH Aachen University, Germany
[2] Institute of Forming Technology and Lightweight Construction, TU Dortmund, Germany

Abstract

The combination of quasi-static and electromagnetic pulse forming increases the formability of sheet metal forming processes. A cooperation between the institute of Applied Mechanics (IFAM) of the RWTH Aachen and the Institute of Forming Technology and Lightweight Construction (IUL) of the TU Dortmund is investigating these processes both experimentally and by simulation for the deep-drawing process of a cross-shaped cup. Aim of the work is to show and prove that with this forming strategy we obtain a more sharpened radius of the cup edges.The combined deformation process is simulated by means of finite elements using a material model developed in [1,2]. A recently proposed finite strain anisotropic viscoplastic model, taking combined nonlinear kinematic and isotropic hardening into account, is coupled with ductile damage in the context of continuum damage mechanics. For the simulation, the evolution equations for the internal variables of the constitutive model are numerically integrated in an explicit manner and the model is then implemented as a user material subroutine in the commercial finite element package LS-Dyna.

Keywords

Modelling, Deep drawing, Damage

1 Introduction

To cope with the ever higher complexity of new sheet metal designs is a challenge. Focusing on the reduction of the weight of parts and the emission during the production leads to improved forming strategies [3]. A major issue is the insufficient formability at

room temperature. To increase the forming limits, the application of combined forming processes is well established [4]. In a study [5], five different low cost, low carbon, low alloy steels are investigated for the effect of high impact velocities of 50 to 220 m/s. It is proven that there are no large differences in ductility observed in quasi-static deformation processes. The ductility at high speed is in the same range. Furthermore, investigations on the increasing formability of the sheet metal forming process due to high strain rates are reported in [6]. In the present work, the process chain on a cross-shaped cup has been investigated. Therefore, an experimental setup has been constructed which leads to a design to combine a standard quasi-static deep drawing forming process with an electromagnetic pulse forming operation.

Nowadays, it is possible to predict and simulate material behaviour by finite element methods. The simulation of this complex combined forming process chain requires a material model which involves all important characteristics. Here, we use a viscoplastic model, based on the multiplicative decomposition of the deformation gradient in the context of hyperelasticity. The kinematic hardening component represents a continuum extension of the classical rheological model of Armstrong-Frederick kinematic hardening. Hill-type plastic anisotropy is modelled by expressing the yield surface as a function of second-order structure tensors as additional tensor-valued arguments. The coupling of damage and plasticity is carried out in a constitutive manner according to the effective stress concept.

The simulation is performed in two steps. First, a slow, quasi-static cross-shaped deep drawing is carried out, during which both plastic deformation and damage evolve in the sheet metal blank. Second, a fast, electromagnetic forming step is simulated. Here, the deformation of the blank is driven by the Lorentz force which results from the interaction of electrical current generated in the blank with a magnetic field generated by a coil in the punch. The results show that an increase in the forming capacity can be achieved by the superposition of a high speed forming step after a conventional quasi-static deep drawing step.

2 Experimental Investigation

2.1 Experimental Setup

The experimental setup is shown in Figure 1a. This setup was used for the realization of the process chain on a cross-shaped cup. A steel punch was used for the quasi-static deep drawing operation. For the following electromagnetic forming, this punch had to be replaced by a punch including coil windings (Figure 1b). The windings are the dies of the electromagnetic forming operation. For them to function, the interface seen in Figure 1a conveys a highly damped alternating current from a capacitor.

The cups were first drawn to 50 mm drawing depth. The drawing radius of the draw ring was 10 mm. The punch had a 20 mm edge radius. During the following electromagnetic forming, the edge radius of the cup is formed further and calibrated. The calibration does not take place along the whole edge. The region, in which no calibration takes place, is shown in Figure 1b. As a result of the calibration, the cup edge is sharpened. A comparison between the calibrated and non-calibrated edges is given In Figure 1c.

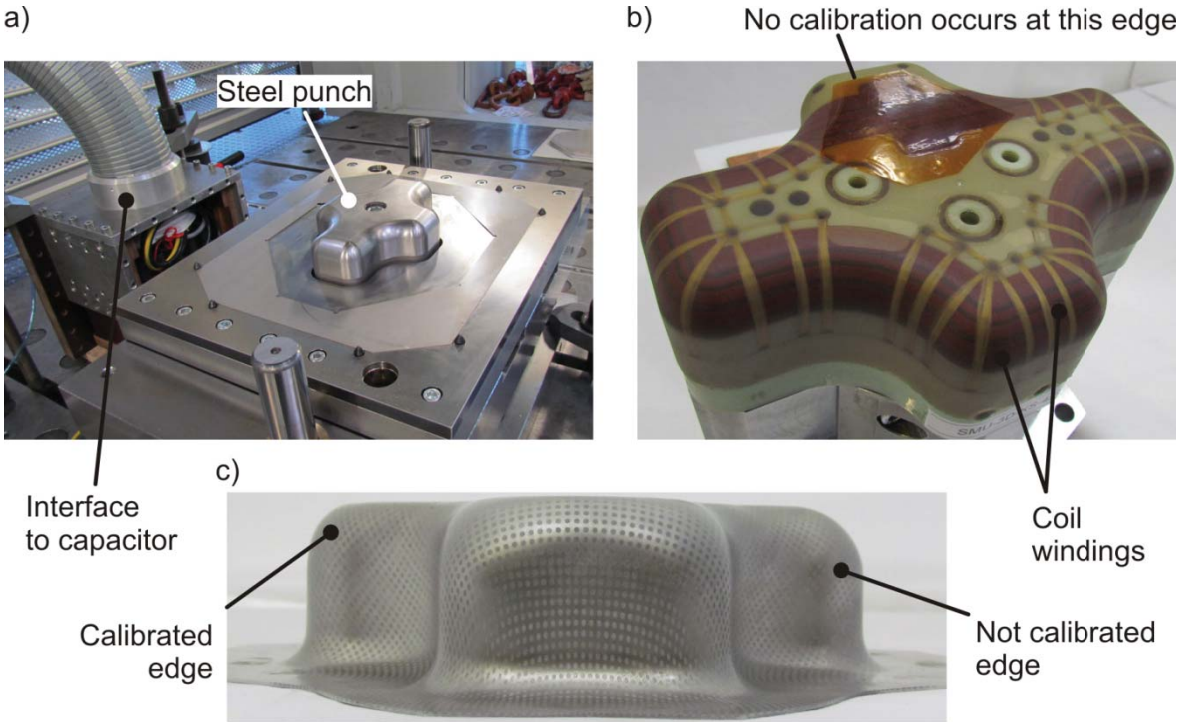

***Figure 1**: a) Experimental setup to realize the process chain on cross-shaped cups b) The punch head with coil windings for electromagnetic calibration at the punch edges c) A comparison between the calibrated and non-calibrated edges*

2.2 Material Characterization

The quasi-static flow curve and the Lankford coefficients of the material aluminum EN AW 5083 were obtained by standard tensile tests. For the flow curves at high strain rates, high speed tensile tests were performed at the company Nordmetall GmbH [7]. The strain rate reached in these experiments was about 1000 s^{-1}. The experiments showed a negligible difference between quasi-static and high-speed flow curves. Hence, the quasi-static flow curves were used for simulations of both deep drawing and electromagnetic forming.

3 Simulation Results

3.1 Material Modelling

A continuum mechanical extension of the classical rheological model of Armstrong-Frederick kinematic hardening can be achieved by the triple multiplicative split $\mathbf{F} = \mathbf{F}_\mathrm{e}\,\mathbf{F}_\mathrm{pe}\,\mathbf{F}_\mathrm{pi}$ of the plastic deformation gradient into “elastic” and “inelastic” parts [8].

The Helmholtz free energy per unit undeformed volume ψ is additively decomposed into the three parts $\psi = \psi_\mathrm{e}(\mathbf{C}_\mathrm{e}) + \psi_\mathrm{kin}(\mathbf{C}_\mathrm{pe}) + \psi_\mathrm{iso}(\kappa)$. The macroscopic elastic material properties are described by the first part ψ_e. The second term ψ_kin corresponds to the elastic energy stored in dislocation fields due to kinematic hardening and vanishes if the kinematic hardening is zero. The third term represents elastic energy due to isotropic

hardening, where κ is the isotropic hardening variable. The Helmholtz free energy is a function of the elastic right Cauchy-Green tensor $\mathbf{C}_\mathrm{e} = \mathbf{F}_\mathrm{e}^\mathrm{T}\mathbf{F}_\mathrm{e} = \mathbf{F}_\mathrm{p}^{-\mathrm{T}}\mathbf{C}\mathbf{F}_\mathrm{p}^{-1}$ and the elastic part of the plastic right Cauchy-Green tensor defined as $\mathbf{C}_\mathrm{pe} = \mathbf{F}_\mathrm{pe}^\mathrm{T}\,\mathbf{F}_\mathrm{pe} = \mathbf{F}_\mathrm{pi}^{-\mathrm{T}}\mathbf{C}\mathbf{F}_\mathrm{pi}^{-1}$. Inserting this in the Clausius-Duhem inequality $-\dot{\psi} + \mathbf{S}\cdot(1/2)\dot{\mathbf{C}} \geq 0$ results in a relation for the second Piola-Kirchhoff stress tensor $\mathbf{S}$. The derivation of the material model is suitably carried out in the intermediate configuration. For the numerical implementation of the constitutive equations it is, however, more appropriate to work in the undeformed or reference configuration. The material model is summarized as follows.

• Second Piola-Kirchhoff stress tensor

$$\mathbf{S} = \frac{1}{1-\mathrm{D}}\,2\mathbf{F}_\mathrm{p}^{-1}\frac{\partial\psi_\mathrm{e}}{\partial\mathbf{C}_\mathrm{e}}\mathbf{F}_\mathrm{p}^{-\mathrm{T}} \tag{1}$$

Here D denotes the isotropic ductile damage variable. Its evolution equation is defined in eq. (5).

• Back stress tensor

$$\mathbf{X} = 2\mathbf{F}_{\mathrm{p_i}}^{-1}\frac{\partial\psi_\mathrm{kin}}{\partial\mathbf{C}_{\mathrm{p_e}}}\mathbf{F}_{\mathrm{p_i}}^{-\mathrm{T}} \tag{2}$$

• Stress-like quantities

$$\mathbf{Y} = \mathbf{C}\mathbf{S} - \mathbf{C}_\mathrm{p}\mathbf{X}, \quad \mathbf{Y}_\mathrm{kin} = \mathbf{C}_\mathrm{p}\mathbf{X} \tag{3}$$

Y is a stress-like quantity variable resulting from the pullback of the Mandel type tensor into the reference configuration.

• Evolution equations

$$\dot{\mathbf{C}}_\mathrm{p} = \dot{\lambda}\frac{\mathrm{sym}(\mathbf{C}_\mathrm{p}(\bar{\mathbf{A}}[(\mathbf{Y}^\mathrm{D})^\mathrm{T}]+(\bar{\mathbf{A}}^\mathrm{T}[\mathbf{Y}^\mathrm{D}])^\mathrm{T})^\mathrm{D}}{\sqrt{\mathbf{Y}^\mathrm{D}\cdot(\bar{\mathbf{A}}[(\mathbf{Y}^\mathrm{D})^\mathrm{T}]}}, \quad \dot{\mathbf{C}}_{\mathrm{p_i}} = 2\dot{\lambda}\frac{\mathrm{b}}{\mathrm{c}}\mathbf{Y}_\mathrm{kin}^\mathrm{D}\mathbf{C}_{\mathrm{p_i}}, \quad \dot{\kappa} = \sqrt{\frac{2}{3}\dot{\lambda}} \tag{4}$$

The superscript D denotes the deviator part of a tensor, $\dot{\lambda}$ is the plastic multiplier and the square brackets denotes the mapping of the second-order tensor by means of the fourth-order tensor $\bar{\mathbf{A}}$. $\mathbf{C}_{\mathrm{p_i}}$ is inelastic plastic part of the right Cauchy-Green tensor. The isotropic hardening variable is defined by κ.

• Scalar isotropic ductile damage variable

$$\dot{\mathrm{D}} = \dot{\lambda}\sqrt{\frac{2}{3}}\frac{1}{1-\mathrm{D}}\left(\frac{\mathrm{Y}}{\mathrm{s}}\right)^\mathrm{k}\mathrm{H}_{(\kappa-\mathrm{p_D})} \tag{5}$$

Y is the strain energy density release rate and p_D the damage threshold. The step function H is equal to one for $\kappa \geq p_D$ and is zero for $\kappa < p_D$.

• Yield function

$$\Phi = \sqrt{\mathbf{Y}^D \cdot (\bar{\mathbf{A}}[(\mathbf{Y}^D)^T])} - \sqrt{\frac{2}{3}}(\sigma_y + Q(1 - e^{-\beta\kappa})) \tag{6}$$

• Slip rate with Perzyna formulation

$$\dot{\lambda} = {\langle\Phi\rangle^m}/{\eta} \tag{7}$$

According to the effective stress concept the second Piola-Kirchhoff stress tensor is modified [1, 2]. The material parameters of the model include the elastic Lamé parameters Λ and μ, the initial yield stress σ_y, the kinematic hardening parameters b and c, isotropic hardening parameters Q and β, Hill's coefficients F, G, H, L, M, N, the damage parameters $s,\ k,\ p_D$ and the viscosity parameter η, $m = 1$.

3.2 Parameter Identification

A uniaxial quasi-static tension test of the aluminum EN AW 5083 has been used for the validation of the material parameters of the presented viscoplastic material model. In a first step, the isotropic parameters are identified based on experimental results with which we have obtained a very good matching as shown in Figure 2a. For $\eta = 0.005$, the two curves are almost equal. In a second step, we have investigated the sensitivity of the model with respect to the viscosity parameter by varying η. As expected, we observe higher stress levels with increasing η. Furthermore, the damage behaviour is investigated here for several parameter combinations. Since there is no experimental data available yet, the investigations are performed numerically. With varying set of parameters, you can see several ways to influence the evolution of damage. Results are shown in Figure. 2b.

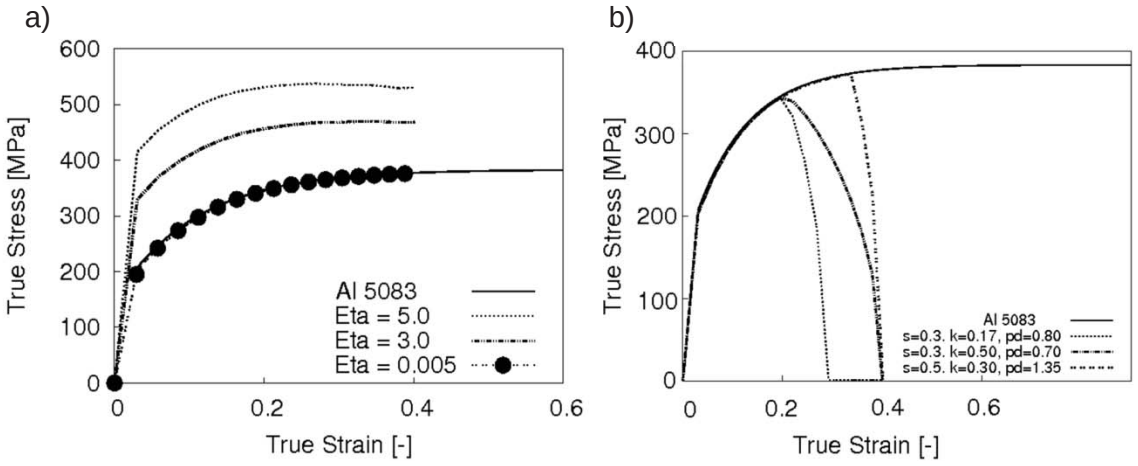

***Figure 2**: a) Stress-strain diagram for different η, b) Stress-strain diagram for different damage parameters s, k, p_D*

3.3 Finite Element Simulation

The previously described experimental setup has been transferred into a finite element model. A quarter model due to symmetry was used for the simulations where tools and dies were modelled as rigid bodies. As the friction coefficient between the workpiece and the die $\mu_{\mathrm{fric}} = 0.06$ was used. 26820 brick elements with 8 nodes and single integration points have been used to model the blank. The deep drawing simulation was performed using the three-dimensional (3D) explicit finite element solver of the commercial software LS-DYNA.

The simulation of the following electromagnetic forming represents a coupled field problem which consists of an electromagnetic and a mechanical part. The electromagnetic problem was solved by the 3D electromagnetic module of the commercial software ANSYS. Then, the mechanical problem was handled with the LS-DYNA explicit solver. A step-by-step coupling between the two solvers was performed by an in-house code developed at the IUL of TU Dortmund. The final setup is shown in Figure 3.

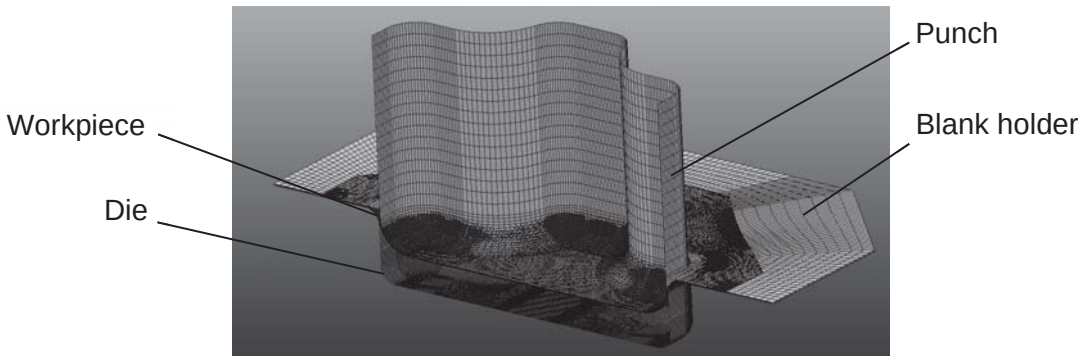

***Figure 3**: Simulation assembly*

The simulation of the coupling of both quasi-static and electromagnetic forming processes is a major issue and has been solved in two steps. At first, the standard deep drawing process is done in a quasi-static manner. When we reach the final punch stroke at the end of the simulation, the stresses and strains are transferred to the second, electromagnetic forming step. With respect to the user material, we have to take all history variables into account which have to be transferred too. A method which is offered by LS-Dyna is a “dynain” file which contains the output information at any requested step.

As a test case, the method is tried and tested on an academic one element example for tensile loading. At first, the element is under load until reaching a defined total process time. Then the variables are stored and transferred and the second simulation step is continuing from the last deformed state. As shown in Figure 4, the method is working very well.

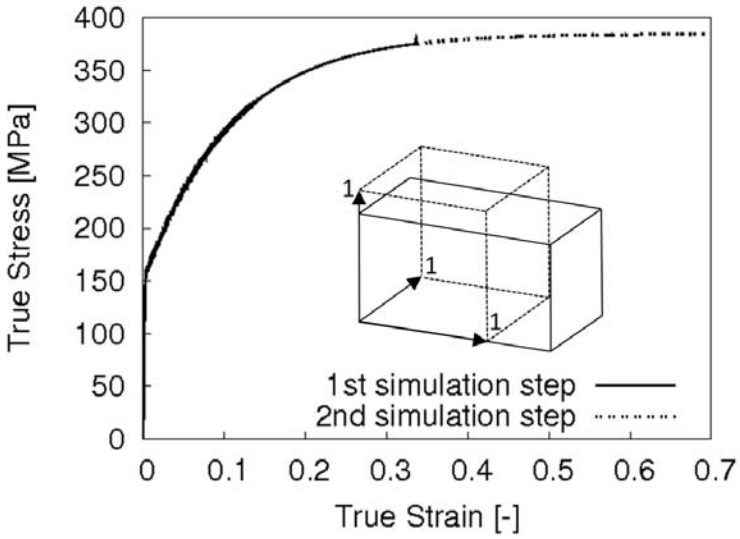

***Figure 4**: Two simulations combined with "dynain" file*

3.4 Results

Next, Figure 5 depicts the final deformed configuration of the blank at the final stage of the punch displacement for the quasi-static deep drawing process. It illustrates exemplary the contour plot of the major strain in a comparison between the experiment and simulation. A good prediction of the critical zones has been achieved.

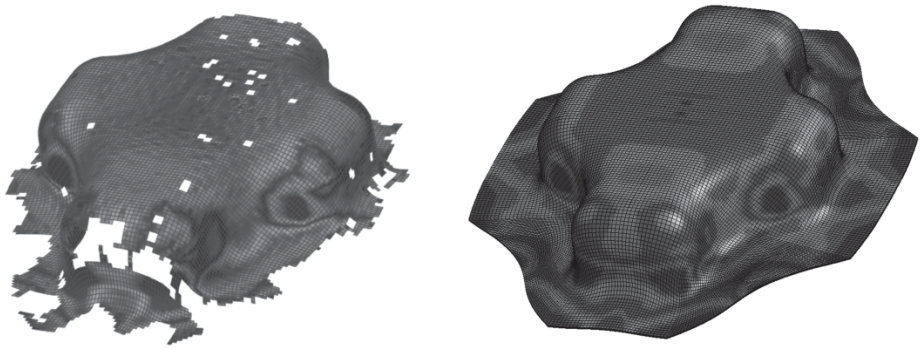

***Figure 5**: Contour plot of the major strain for experiment (left) and simulation (right)*

The measured experimental sample was evaluated for major and minor strains and plotted in a FLD which are represented by crosses in Figure 6a. For the comparison, the most important areas of the deformed blank of the simulation have been taken into account and are represented by the numbered rectangles. Compared to Figure 6b, numbers indicate the measured area of the blank. We can observe here a good correlation to the FLD with the expected strain ratios differ from plain strain to full biaxial.

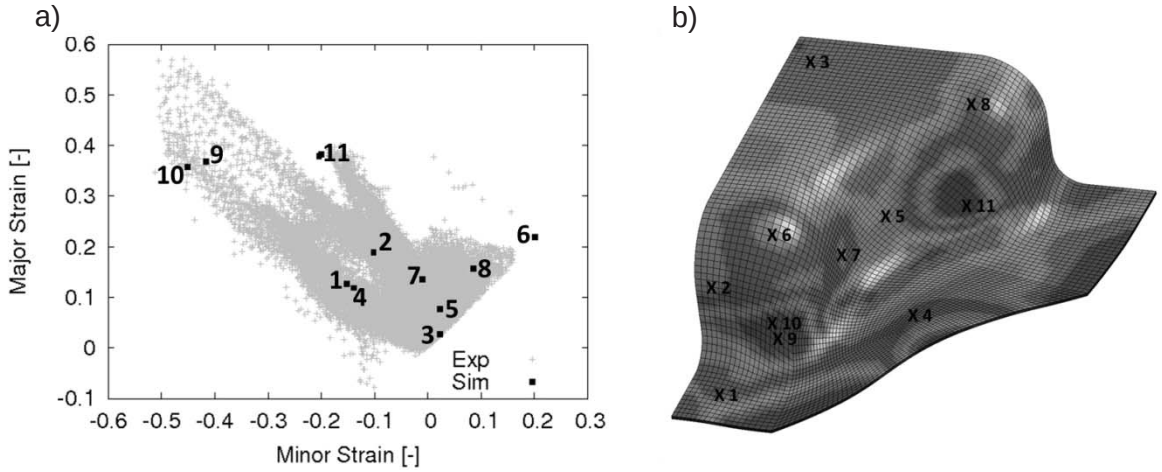

***Figure 6**: Comparison of FLD between experiment and simulation*

As already shown by the experimental investigations which were presented in Figure 1c, an increase of the total deformation is shown in Figure 7 which can be achieved by the superposition of a high speed forming step after a conventional quasi-static deep drawing step. As a result of the simulation, the distribution plot of the equivalent plastic strain after deep drawing and electromagnetic forming depicts a sharpening of the radius on each corner. It shows a good result regarding the formability.

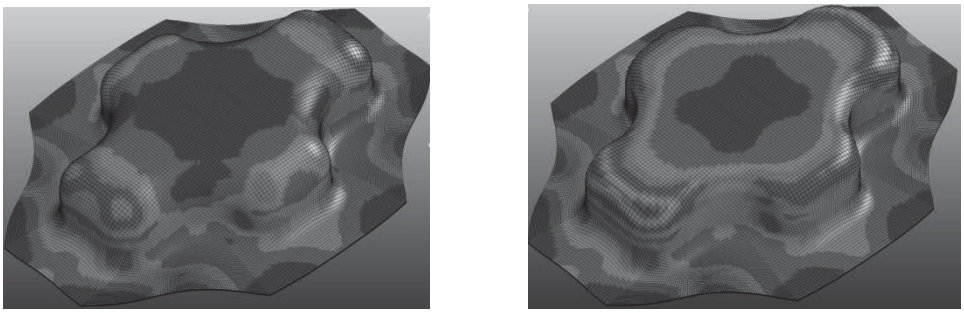

***Figure 7**: Distribution of equivalent plastic strain after (left) deep drawing and (right) electromagnetic forming*

4 Summary

In this paper, we investigate the finite element simulation of the process chain quasi-static deep drawing – electromagnetic forming by means of a new coupled damage-viscoplasticity model for large deformations. For this purpose, a recently proposed finite strain anisotropic viscoplastic model, taking combined nonlinear kinematic and isotropic hardening into account, is coupled with ductile damage in the context of continuum damage mechanics. The coupling of damage and plasticity is carried out in a constitutive manner according to the effective stress concept.

The numerical examples investigate the potential of the constitutive framework regarding the simulation of the forming limits. In particular, the coupled material model is

applied to the combined quasi-static – electromagnetic simulation of the cross-shaped cup deep drawing process. For this purpose, the evolution equations for the internal variables of the constitutive model are numerically integrated in an explicit manner and the model is then implemented as a user material subroutine in the commercial finite element package LS-Dyna. The results show that an increase in the total deformation can be achieved by the superposition of a high speed forming step after a conventional quasi-static deep drawing step.

5 Acknowledgement

This work is based on the results of PAK343 “Methodenplanung für quasistatisch-dynamisch kombinierte Umformprozesse”. The authors would like to thank the “Deutsche Forschungsgemeinschaft (DFG)” for its financial support.

References

[1] Vladimirov, I. N.; Kiliclar, Y.; Tini. V.; Reese, S.: Constitutive modelling of anisotropy, hardening and failure of sheet metals, Key Engineering Materials, 2011, Vol. 473, pp. 631-636.

[2] Vladimirov, I. N.; M. P. Pietryga, M. P.; Reese, S.: Prediction of forming limit diagrams at fracture by an anisotropic finite plasticity model with ductile damage, steel research international, special issue ICTP2011, 2011, pp. 883-888.

[3] *Bull, M.*; Chavakari, R.; Mascarin, A.: Benefit analysis: Use of aluminum structures in conjunction with alternative power-train technologies in automobiles. IBIS Associates, Inc for the Aluminum Association, 2008

[4] Imbert, J. M.; Winkler, S. L.; Worswick, M. J.; Oliveira, D. A.; Golovaschenko, S.: The effect of tool-sheet interaction on damage evolution in electromagnetic forming of aluminum alloy sheet. Journal of Engineering Materials and Technology, 2005, Vol. 127, pp. 145-153

[5] Seth, M; Vohnout, V. J.; Daehn, G. S.: Formability of steel sheet in high velocity impact. Journal of Materials Processing Technology, 2005, Vol. 168, pp. 390-400

[6] Balanethirama, V. S.; Daehn, G. S.: Hyperplasticity: Increased forming limits at high workpiece velocity. Scripta Metallurgica et Materialia, 1994, Vol. 30, pp. 515-520

[7] www.nordmetall.net

[8] Vladimirov, I. N.; M. P. Pietryga, M. P.; Reese, S.: On the modelling of nonlinear kinematic hardening at finite strains with application to springback – comparison of time integration algorithms, International Journal for Numerical Methods in Engineering, 2008, Vol. 75, pp. 1-28